American Mineralogist, Volume 73, pages 534–546, 1988

^{27}Al and ^{29}Si MASS NMR spectroscopy of glasses in the system anorthite-diopside-forsterite

Richard Oestrike,* R. James Kirkpatrick
Mineral Physics Program, Department of Geology, University of Illinois, 1301 W. Green Street, 245 Natural History Building, Urbana, Illinois 61801, U.S.A.

Abstract

^{27}Al and ^{29}Si MASS NMR spectroscopy of glasses in the system anorthite-diopside-forsterite indicates that, within the accuracy of the technique, all Si and Al are tetrahedrally coordinated to oxygen and that most, if not all, of the Al is in fully polymerized (Q^4) sites. Estimates of the average $\overline{Si–O}$ bond length and average $\angle\overline{Si–O–T}$ (T = Si, Al) bond angle determined from empirical correlations of ^{29}Si chemical shift with bond length and angle indicate that these parameters vary from 1.62 Å and 134° for anorthite glass to 1.64 Å and 129° for $Di_{90}Fo_{10}$ glass. ^{29}Si peak maxima and breadths for glasses quenched from above the liquidus are nearly the same as those for glasses quenched from at or below the liquidus, but are slightly more shielded and broader. Model calculations based on the ^{27}Al peak maxima indicate that the abundance of Q^4 sites in glasses along the join An-Di is approximately equal to that of a mechanical mixture of An and Di, whereas glasses along the join Cats-Di (data from Kirkpatrick et al., 1986a) contain more Q^4 sites than expected for a mechanical mixture of Cats and Di. The models also indicate that the average polymerization of the non-Q^4 sites is approximately Q^2 along the An-Di join and approximately $Q^{1.7}$ along the Cats-Di join.

Introduction

This paper presents the results of a high-resolution ^{27}Al and ^{29}Si MASS NMR spectroscopic study of the structure of glasses in the basalt-analogue system anorthite-diopside-forsterite ($CaAl_2Si_2O_8$-$CaMgSiO_6$-Mg_2SiO_4; An-Di-Fo) and additional interpretation of the ^{27}Al MASS NMR data for glasses along the join $CaAl_2SiO_6$-$CaMgSiO_6$ (Cats-Di; Kirkpatrick et al., 1986a). The data are interpreted by comparison to the MASS NMR data for crystals (e.g., Kirkpatrick et al., 1985a, and references therein), the data for tetrahedral framework glasses (DeJong et al., 1984; Murdoch et al., 1985; Oestrike et al., 1987b), and the data for the system CaO-Al_2O_3-SiO_2 (Engelhardt et al., 1985).

Knowledge of melt structure is necessary to understand and predict such physical properties of melts as density and viscosity, crystal-liquid phase equilibria, diffusivities and the mechanisms of diffusion, and the mechanisms of nucleation and crystal growth. Quenched-glass samples rather than melts have been used in this study, because our NMR spectrometers are not at present equipped to observe high-temperature, molten samples. Several studies utilizing a variety of techniques, including X-ray scattering, Raman spectroscopy, and physical property measurements, have failed to detect major structural differences between aluminosilicate glasses and melts of the same composition (Riebling, 1967; Waseda and Toguri, 1977; Taylor et al., 1980; Seifert et al., 1981; Domine and Piriou, 1983), despite the rapid change in heat capacity at glass transition temperatures (Carmichael, 1979; Navrotsky, 1981; Angell, 1985). Thus, it is likely that the nearest-neighbor (NN) and next-nearest-neighbor (NNN) structural information obtained for glasses via NMR spectroscopy is applicable to melt structure.

The An-Di-Fo glasses studied here have compositions falling in the primary phase fields of anorthite, diopside, forsterite, and spinel (Osborn and Tait, 1952). Several compositions along the join An-Di were also quenched from a variety of superheatings and supercoolings after programmed cooling to investigate the effect of different thermal histories on their structures (Richet and Bottinga, 1984; Brawer, 1985; Navrotsky, 1986).

Because glasses do not have long-range order and because NMR and other spectroscopic techniques are most sensitive to NN and NNN structure, we interpret the data for these glasses in terms of Si and Al tetrahedral sites rather than extended structures (e.g., frameworks, sheets, chains). ^{29}Si and ^{27}Al MASS NMR spectroscopy yields the following information about Si and Al sites in glasses: (1) the nearest-neighbor coordination number(s) and an estimate of the proportions of each, (2) the polymerization state(s) of the silica and alumina tetrahedra and an estimate of the proportions of each, and (3) the average mean Si–O bond length per tetrahedron ($\overline{Si–O}$) and average mean Si–O–T (T = Si, Al) bond angle per tetrahedron ($\angle\overline{Si–O–T}$).

The Si and Al coordination and the Al polymerization

* Present address: 39 Crescent Road, Poughkeepsie, New York 12601, U.S.A.

0003–004X/88/0506–0534$02.00

can be obtained from NMR peak positions (Kirkpatrick et al., 1985a, and references therein). The Si and Al polymerization can also be examined by modeling the ^{27}Al spectra (this study). $\overline{\text{Si–O}}$ and $\angle\overline{\text{Si–O–T}}$ can be obtained by comparison of ^{29}Si spectra with published empirical correlations.

Previous work

We briefly review here those aspects of glass structure relevant to the present investigation and the results of recent high-resolution NMR investigations of crystals and glasses necessary for the interpretation of our data. For more comprehensive discussions of glass structure, see the recent reviews of McMillan (1984a), Navrotsky (1986), Richet and Bottinga (1986), Brawer (1985), Bray (1985), and Kirkpatrick et al. (1986b).

Glass structure

Si has long been accepted to be in tetrahedral coordination to oxygen in aluminosilicate glasses prepared at 1-atm pressure (Randall et al., 1930). The coordination of Al in aluminosilicate glasses prepared at 1-atm pressure has been controversial, with 4-, 5-, and 6-fold coordination to oxygen as well as Al "triclusters" (Lacey, 1963) considered possible. Many studies show that aluminosilicate glasses with M/Al $\geq$ 1 (M = one monovalent or one-half a divalent cation) prepared at 1-atm pressure contain only tetrahedral Al (e.g., Taylor and Brown, 1979a, 1979b; Mysen et al., 1981), although it has recently been suggested that this may not be true if B is present (Dupree et al., 1985; Oestrike et al., 1987a). There is also wide agreement that at least some aluminosilicate glasses with M/Al < 1 contain both tetrahedral (^{IV}Al) and octahedral Al (^{VI}Al). Five-coordinate Al (^{V}Al) may also be present (Risbud et al., 1987).

Si and ^{IV}Al polymerize in melts and glasses to produce tetrahedral sites with from zero to four oxygens bridging to neighboring tetrahedra (Q^0 to Q^4 sites). Numerous studies indicate that Si tetrahedra in glasses normally occur in more than one polymerization state and that the distribution of polymerization states is a function of composition (e.g., Mysen et al., 1982; Dupree et al., 1984). Recent work has indicated that ^{IV}Al is strongly partitioned into the most polymerized sites (Mysen et al., 1981, 1985; Domine and Piriou, 1986). Because spectroscopic techniques for the most part yield information about only the local structural environment, it is at present unclear whether sites of a given polymerization are isolated or occur as clusters of similar sites forming larger fragments. Potentially useful techniques to investigate this intermediate-range structure of glasses are discussed by Angell (1985).

High-resolution NMR spectroscopy of crystals and glasses

Because it is not yet possible to calculate from first principles the NMR chemical shift for an assumed structural arrangement, information about the structures of poorly known substances such as glasses can only be obtained by comparison with MASS NMR data for materials with known structures. Thus, we briefly review here the relevant high-resolution NMR data for crystals.

For crystalline silicates, the ^{29}Si chemical shift becomes more negative (more shielded) as the polymerization increases (Lippmaa et al., 1980), but the ranges of ^{29}Si chemical shifts for particular classes of silicate structures overlap significantly (K. A. Smith et al., 1983). Substitution of Al for Si in the tetrahedral sites of framework and sheet silicates causes the ^{29}Si chemical shift to become less negative (less shielded) by 3–5 ppm per Al NNN (Lippmaa et al., 1981; Kinsey et al., 1985). The counteracting effects of increasing polymerization and increasing tetrahedral Al content make interpretation of ^{29}Si chemical shifts for aluminosilicate materials with poorly known structures difficult.

The ^{29}Si chemical shift correlates with several structural bonding parameters in crystals. These parameters include $\angle\overline{\text{Si–O–T}}$ (J. V. Smith and Blackwell, 1983; Kirkpatrick et al., 1985a), $\overline{\text{Si–O}}$ bond distance (Higgins and Woessner, 1982; J. V. Smith and Blackwell, 1983; K. A. Smith et al., 1983; J. V. Smith et al., 1984), the sum of the Brown and Shannon (1973) bond strengths (K. A. Smith et al., 1983), and the group electronegativity (Janes and Oldfield, 1985).

Another important result of ^{29}Si MASS NMR spectroscopy of crystals is that it is possible to resolve signals from Si atoms with different numbers of Al NNN in the same phase. Si-Al disorder in zeolites has been studied in this way by numerous workers (e.g., Fyfe et al., 1982a, 1982b; Thomas et al., 1983a, 1983b).

The interpretation of ^{27}Al MASS NMR data is complicated by second-order quadrupolar effects, including peak broadening and displacement of the peak to more shielded values than the isotropic chemical shift (Ganapathy et al.,1982; Kirkpatrick et al., 1985b). Using ^{27}Al MASS NMR, it is easy to distinguish ^{IV}Al from ^{VI}Al (Müller et al., 1981; Fyfe et al., 1982a; Kinsey et al., 1985). At an $\mathbf{H}_0$ magnetic field strength of 11.7 T, the range of ^{27}Al peak maxima for aluminosilicates is from about +50 to +80 ppm for ^{IV}Al and from −10 to +20 ppm for ^{VI}Al (Kirkpatrick et al., 1985a). In addition, ^{27}Al peak maxima for ^{IV}Al in framework silicates fall in the range +50 to +65 ppm, whereas those for ^{IV}Al in sheet silicates fall in the range +65 to +75 ppm. ^{27}Al peak maxima for ^{IV}Al in aluminates typically fall in the range of +75 to +80 ppm. For ^{IV}Al in framework silicates and aluminates and in sheet silicates there appear to be trends of more-positive peak maxima (decreased shielding) with decreasing Si/(Si + ^{IV}Al). These trends parallel the trend of the ^{29}Si chemical shifts.

Also, because of the quadrupolar behavior of ^{27}Al, signal from sites with large quadrupole coupling constants (QCCs) can be lost because of rapid decay of the signal in the 7- to 20-μs delay time between the end of the radiofrequency pulse and the beginning of the collection of the data (pulse-breakthrough period). Theoretical un-

TABLE 1. Electron-microprobe analyses (wt%) of glasses studied

An:Di:Fo (wt%)	CaO	MgO	Al_2O_3	SiO_2	Total
100:0:0	19.98	0.00	35.50	43.90	99.39
80:20:0	21.09	3.55	29.16	46.41	100.21
60:40:0	22.22	7.11	22.02	48.60	99.95
40:60:0	22.74	10.62	15.05	51.86	100.27
20:80:0	24.65	14.39	7.68	53.84	100.55
15:85:0	24.88	14.42	7.66	53.31	100.26
10:90:0	24.72	16.49	3.95	54.46	99.63
80:10:10	18.37	8.27	28.90	44.25	99.79
60:30:10	19.76	11.67	21.49	47.09	100.01
50:40:10	19.71	13.62	18.55	49.18	101.06
40:50:10	20.55	15.34	14.72	49.65	100.26
20:70:10	21.69	19.29	7.57	52.46	101.01
10:80:10	22.04	21.13	3.99	53.72	100.88
80:0:20	15.80	12.82	28.29	43.90	100.81
60:20:20	16.72	16.22	21.45	46.00	100.38
40:40:20	17.59	19.69	14.73	48.66	100.67

TABLE 2. Experimental conditions for samples not quenched from within 5 °C of the liquidus

An:Di:Fo (wt%)	Liquidus* (°C)	Initial temp. (°C)	Cooling rate (°C/h)	Quench temp. (°C)	Experiment no.
100:0:0**	1391	1471	2.5	1300	1
100:0:0**	1391	1471	100	1250	2
100:0:0**	1391	1471	1000	1400	3
100:0:0**	1391	1471	1000	1300	4
100:0:0**	1391	1471	1000	1200	5
20:80:0	1343	1393	w.q.†	1393	6
20:80:0	1343	1543	w.q.†	1543	7
20:80:0	1343	1353	2.5	1303	8
40:60:0	1282	1530	w.q.†	1530	9
60:40:0	1388	1398	2.5	1323	10

Note: Temperature accuracy is ±5 °C.
* Liquidus temperatures after Osborn and Tait (1952).
** Samples provided by Y. Aoki.
† Water quench.

derstanding of why a given amount of signal is lost under different run conditions is incomplete (Schmidt, 1971; Fenzke et al., 1984). Kirkpatrick et al. (1986a), however, reported a method to quantitatively determine the amount of ^{27}Al signal detected and showed that, within the accuracy of the technique (10–15%), all Al signal is detected in their spectra of Di-Cats glasses. We have used this technique for the An-Di-Fo glasses studied here.

The variations of ^{27}Al and ^{29}Si NMR chemical shifts of glasses generally parallel those of crystals. The peaks for glasses are broader than for crystals (see Kirkpatrick et al., 1986b, for a review), and except for alkali silicate glasses (e.g., Dupree et al., 1984), separate peaks for different types of Si sites cannot normally be resolved. With respect to this study, the most important results for glasses are the following:

1. For framework glasses (those with M/Al = 1), the ^{27}Al and ^{29}Si chemical shifts become less shielded with decreasing Si/(Si + Al) (Oestrike et al., 1987b). These relationships parallel those of the crystals. We will use this relationship for ^{27}Al to help interpret the structure of the An-Di-Fo glasses.

2. For compositions with M/Al > 1, at constant mole percent SiO_2, the ^{29}Si chemical shift becomes less shielded as M/Al increases, reflecting the increasing number of nonbridging oxygens (Engelhardt et al., 1985).

EXPERIMENTAL METHODS

Sample preparation

Glasses were prepared by fusion of 99.999% pure oxide-carbonate mixtures in Pt crucibles. Two- to five-gram starting batches of each composition (Table 1) were fused at least three times at 50 to 100 °C above their liquidus temperatures for 1–2 h and quenched. Between fusions, each sample was ground with an agate mortar and pestle. One-gram aliquots of these batches for spectroscopic examination were then fused for 1 h within 5 °C of the liquidus temperature and quenched by immersing the bottom of the Pt crucible in water. Estimated cooling time is about 4 s, yielding average cooling rates of 250 to 400 °C/s.

To determine whether NMR spectroscopy can detect structural differences in glasses with different thermal histories, representative compositions were examined after different thermal treatments. Aliquots of glasses with the compositions (wt%) $An_{10}Di_{80}Fo_{10}$, $An_{40}Di_{40}Fo_{20}$, $An_{30}Di_{50}Fo_{20}$, and $An_{20}Di_{80}$ that had been produced at 50 to 100 °C above their liquidi were heated at 50 °C above their liquidi for 1 h and then quenched by immersing the bottom of the crucible in water. Aliquots of $An_{20}Di_{80}$ and $An_{40}Di_{60}$ were heated for 1 h at 200 °C and 250 °C above their liquidi, respectively, and quenched in the same way. Additional aliquots of $An_{60}Di_{40}$, $An_{40}Di_{60}$, $An_{20}Di_{80}$, and Di_{100} were heated above their liquidi for 1 h (1.5 h for experiment 6, Table 2) and then quenched or programmed cooled (see Table 2 for heating and quenching conditions).

Homogeneity and correctness of composition were checked using a JEOL model JXM-50A electron microprobe operating at 20 keV with a beam current of 300 pA. Counting time was 120 s, and the beam diameter was 1–2 μm. Data correction was made with a MAGIC-type program. Table 1 gives analyses of these glasses, which all have their nominal composition within the analytical uncertainty. All are homogeneous and free of crystals.

Spectroscopy

The NMR spectra were obtained with home-built NMR spectrometers at field strengths of 8.45 and 11.7 T using the instruments and methods described by K. A. Smith et al. (1983) and Kirkpatrick et al. (1985b). Home-built sample probes with Andrew-Beams type rotors (Andrew, 1971) were used.

Peak positions are reported as the parts-per-million (ppm) deviation of the sample resonance frequency from that of a standard; the deviation is referred to as the chemical shift. For ^{29}Si, the standard used in this study is hexamethyldisiloxane (HMDS) in $Cr(acac)_3$-doped CH_2Cl_2 (K. A. Smith et al., 1983). The HMDS chemical shift is taken as +6.6 ppm from tetramethylsilane (TMS), which has a chemical shift of 0 ppm by convention. The ^{27}Al standard is 1*M* $AlCl_3$ solution, which also has a chemical shift of 0 ppm by convention. Less positive or more negative chemical shifts indicate greater shielding.

The orientation of the rotor spin axis was set to the magic angle by maximizing the spinning-sideband intensities for $K^{79}Br$ and $K^{127}I$ for ^{27}Al and ^{29}Si, respectively. Spinning speed was determined by measuring the frequency difference between spinning sidebands of the ^{79}Br or ^{127}I spectra.

Peak broadening due to field drift, field inhomogeneity, and rotor wobble is estimated to be at most 200 Hz at half-height (1.5 ppm for ^{27}Al; 3.0 ppm for ^{29}Si) and more typically about

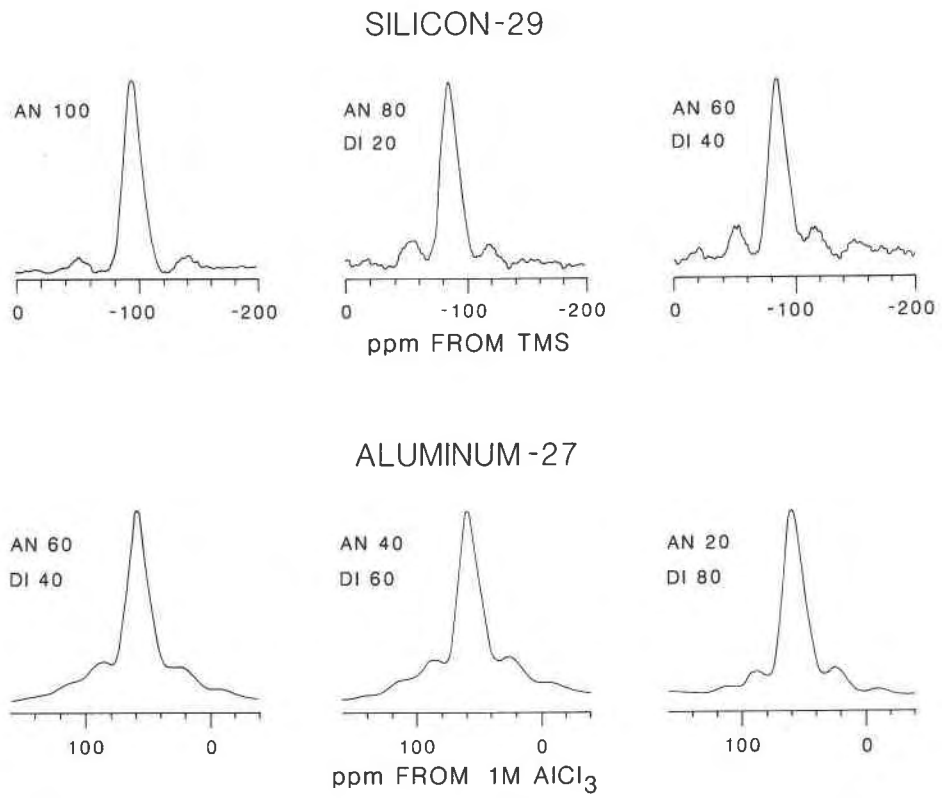

Fig. 1. 8.45-T ^{29}Si and 11.7-T ^{27}Al MASS NMR spectra of An-Di-Fo glasses. For ^{27}Al, note the lack of signal at about 0 ppm, which would indicate ^{VI}Al.

100 Hz. This value is far less than the peak widths of the glasses described here (typically 800 to 3000 Hz). This peak broadening has not been removed from the reported peak breadths, but peak broadening due to use of exponential multipliers (which greatly increase the signal-to-noise ratio but also artificially increase peak width) has been removed.

The peak positions for both ^{27}Al and ^{29}Si are taken to be the chemical shift at maximum intensity. Owing to the large peak breadths and phasing errors, peak positions are reported to only ± 1 ppm.

In addition, because of unaveraged second-order quadrupole effects, the ^{27}Al peak position does not correspond to the isotropic chemical shift. Instead it is displaced to more shielded values (to the right in our spectra) an unknown amount that depends primarily on the average ^{27}Al QCC. Because the glasses are disordered and contain a range of Al sites, simulation of the spectra to obtain QCCs in the manner of Ganapathy et al. (1982) and Kirkpatrick et al. (1985b) is not possible. The magnitude of peak displacement is not well known, but the differences in peak maxima at 11.7 and 8.45 T indicate that it is likely to be of the order of 1 to 3 ppm at 11.7 T. Because the magnitude of displacement of the peak position decreases with increasing field strength, all interpretations of ^{27}Al in this paper use only data obtained at 11.7 T.

We calculate below bond angles and bond distances for the glasses using correlations of the ^{29}Si chemical shift with these parameters for crystalline silicates. Errors in the calculated values for the glasses arise from two sources: errors in measurement of the ^{29}Si chemical shift and errors in the position of the least-squares correlation line. In addition, we must make the assumption that the correlations for crystals apply to glasses. The errors produced by inaccurate placement of the correlation line are assessed by calculating the 95% confidence band for the position of the correlation line (Wonnacott and Wonnacott, 1970). The total error reported is the sum of the errors due to inaccuracy of measurement and inaccuracy of correlation at the 95% confidence level.

RESULTS

Samples quenched from near-liquidus temperatures

The ^{29}Si and ^{27}Al spectra of all the An-Di-Fo glasses contain broad, featureless central peaks along with smaller peaks that are spinning sidebands due to MASS (Fig. 1). Table 3 lists the ^{29}Si peak maxima, FWHHs, base coordinates, and the ratio of nonbridging oxygens to tetrahedral cations (NBO/T). Table 4 lists the ^{27}Al peak maxima for all the samples quenched from near the liquidus. The positions of the left and right bases of ^{29}Si peaks can be difficult to determine and are not usually reported. We list them here to give some idea of the full range of chemical shifts. The bases of the ^{27}Al peaks cannot be determined because of overlap with the spinning sidebands.

The ^{29}Si peak maxima for the samples quenched from the liquidus all fall in the range -80 to -88 ppm, consistent with their relatively low Si/(Si + Al) ratios and (for many) depolymerized compositions. For crystals, this chemical shift range is typical of Q^2, Q^3, Q^4(4Al) sites (Q^4

TABLE 3. ^{29}Si MASS NMR data for anorthite-diopside-forsterite glasses (H_0 = 8.45 T)

An:Di:Fo (wt%)	^{29}Si chemical shift (±1 ppm)	^{29}Si FWHH (±1.5 ppm)	Left base (±4 ppm)	Right base (±4 ppm)	NBO/T
100:0:0	−87.9	15.2	−71	−106	0
80:20:0	−85.9	14.7	−71	−105	0.28
60:40:0	−85.4	14.9	−71	−100	0.60
40:60:0	−83.5	14.9	−68	−101	0.98
20:80:0	−81.5	14.7	−68	−99	1.44
15:85:0	−83.5	15.1	−68	−104	1.57
10:90:0	−81.8	15.8	−67	−100	1.71
0:100:0	−81.6	15.4	−69	−100	2.00
80:10:10	−84.5	14.7	−69	−103	0.36
60:30:10	−84.4	15.1	−71	−104	0.69
50:40:10	−82.0	14.6	−66	−102	0.88
40:50:10	−82.8	14.6	−68	−100	1.09
20:70:10	−80.0	15.4	−64	−103	1.57
10:80:10	−80.8	15.4	−66	−104	1.85
80:0:20	−82.8	14.6	−68	−102	0.44
60:20:20	−81.5	14.2	−67	−99	0.79

TABLE 4. ^{27}Al MASS NMR data for anorthite-diopside-forsterite glasses

An:Di:Fo (wt%)	^{27}Al chemical shift at 11.7 T (±1 ppm)	^{27}Al FWHH at 11.7 T (±1.5 ppm)	^{27}Al chemical shift at 8.45 T (±1 ppm)
100:0:0	58.8	21.8	N.D.
80:20:0	59.0	21.3	59.9
60:40:0	58.6	20.9	57.8
40:60:0	57.9	20.9	56.8
20:80:0	58.1	18.4	57.6
15:85:0	59.9	19.9	N.D.
10:90:0	59.7	17.7	N.D.
80:10:10	62.4	21.7	58.5
60:30:10	59.5	27.4*	59.1
50:40:10	58.6	21.3	58.2
40:50:10	58.4	21.1	58.4
20:70:10	58.6	20.8	58.9
10:80:10	58.8	23.2*	57.9
80:0:20	61.4	19.9	59.9
60:20:20	61.4	19.5	N.D.
40:40:20	61.0	18.4	58.0
30:50:20	59.4	17.8	N.D.

* Extensive overlap with spinning sidebands.

sites with four Al NNN, Kirkpatrick et al., 1985a). These chemical shifts are almost within experimental error of those for glasses with similar Si/(Si + Al) and NBO/T values in the system CaO-Al_2O_3-SiO_2 (Engelhardt et al., 1985). As for most other aluminosilicate glasses, the spectra of our samples do not contain resolvable peaks or shoulders because of different types of sites.

There are several systematic trends of the ^{29}Si peak maxima. At a given Fo content, they become less shielded (less negative) with increasing Di/An. For a given An content, they become less shielded with increasing Fo/Di. For a given Di content, they become less shielded with increasing Fo/An. In each case, deshielding correlates with an increasing NBO/T ratio (Table 3).

The ^{29}Si FWHHs do not vary significantly, and are all within experimental error of 15 ppm.

The 11.7-T ^{27}Al chemical shifts for the samples quenched from the liquidus all fall in the range 57.9 to 62.4 ppm. Most are between 58 and 60 ppm and are identical within experimental error. These values are about 3–5 ppm less shielded (more positive) than those of Engelhardt et al. (1985) for similar CaO-Al_2O_3-SiO_2 glasses. They collected their data at a lower $\mathbf{H}_0$ field strength of 9.45 T, which gives rise to a larger quadrupolar displacement of the peaks. Our data at $\mathbf{H}_0$ = 11.7 T are closer to the isotropic chemical shifts than theirs, because the quadrupole displacement scales as $(1/\mathbf{H}_0)^2$ (Ganapathy et al., 1982). The isotropic ^{27}Al chemical shifts of the CaO + MgO glasses and their CaO glasses with similar Si/(Si + Al) and NBO/T are probably very similar.

The ^{27}Al quantitation experiments using the methods of Kirkpatrick et al. (1986a) show that within experimental error, all the ^{27}Al signal is detected for our samples. Figure 2 is a plot of the intensity of the free induction decay vs. time and shows that the extrapolations of the intensity to t = 0 are very close to the value expected from the theoretical analysis of Fenzke et al. (1984) for a pulse width of ⅙ that of the solution 90° pulse width (the conditions of our experiments; see Kirkpatrick et al., 1986a, for further discussion). Table 5 summarizes the results and shows that for the samples we have examined the detected fraction of the expected signal varies from 0.83 to 1.08 with a mean of 0.94. The values do not vary systematically with composition, and we interpret the results to indicate that we are detecting all or nearly all of the signal. Because of the large extrapolations (about a factor of 3), precision and accuracy of the method is relatively low, about ±0.1 to ±0.15. These results are similar to those for Di-Cats ($CaMgSi_2O_6$-$CaAl_2SiO_6$) glasses (Kirkpatrick et al., 1986a).

Samples quenched from above and below the liquidus

Table 6 lists the ^{29}Si and ^{27}Al NMR data for samples quenched from temperatures significantly above the liquidus and for samples quenched from significantly below the liquidus after programmed cooling. The spectra of these samples are very similar to those in Figure 1 and are not shown. The differences in peak position and peak width between these spectra and those of samples quenched from near the liquidus are at most only slightly more than the estimated uncertainties for peak position and width.

For the superheated samples, the ^{29}Si chemical shifts are on average slightly more negative (more shielded), with the largest change being 1.7 ppm for $An_{40}Di_{60}$ quenched from 250 °C above the liquidus. Di_{100} and $An_{20}Di_{80}$ quenched from 200 °C above the liquidus have peak positions less than 1 ppm more negative, identical within the analytical uncertainty. The ^{29}Si peak widths of the superheated samples are 1.7, 1.4, and 1.2 ppm wider for Di_{100}, $An_{20}Di_{80}$, and $An_{40}Di_{60}$, respectively. The nominal accuracy of the peak-width measurements, however, is about ±1.5 ppm.

The supercooled samples yield slightly less negative (less shielded) ^{29}Si chemical shifts and peak widths that are

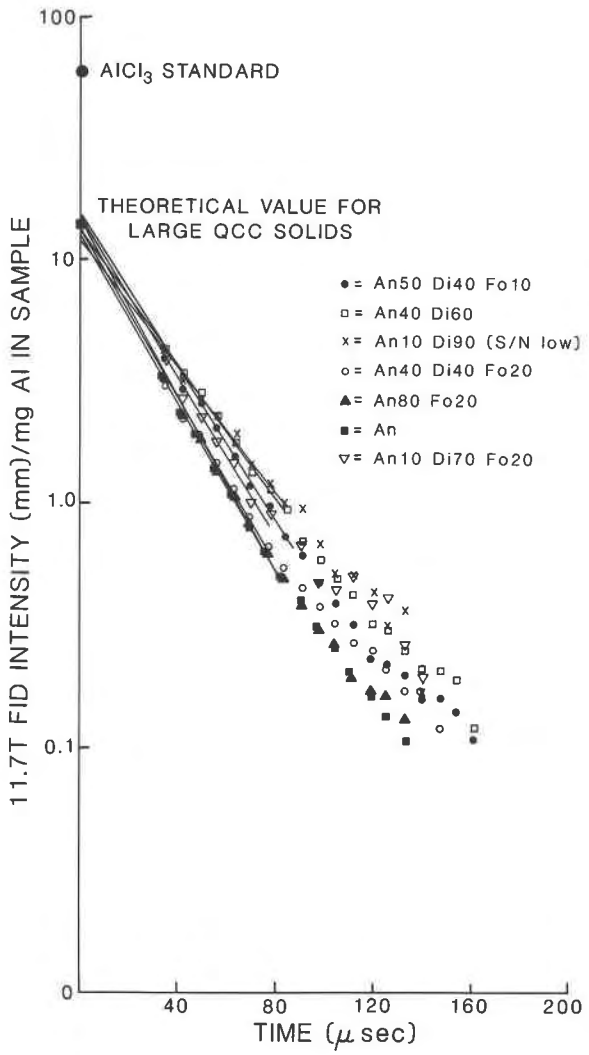

Fig. 2. 11.7-T NMR FID intensity vs. time for ^{27}Al in An-Di-Fo glasses. Extrapolation of these curves to the expected value at $t = 0$ indicates that, within experimental error, all the ^{27}Al signal is being detected. See text for discussion.

not systematically different than those of samples quenched from the liquidus. The largest change in peak position is 1.8 ppm for $An_{60}Di_{40}$. Changes in peak position for Di_{100} and $An_{20}Di_{80}$ are within analytical uncertainty.

All variations in both ^{27}Al peak position and peak width for samples with different thermal histories are within analytical uncertainty, and the small variations observed are not systematic.

Discussion

Samples quenched from the liquidus

Using the ^{27}Al and ^{29}Si MASS NMR data for the An-Di-Fo glasses, published results for the MASS NMR behavior of silicate and aluminosilicate crystals and glasses, and published interpretations of aluminosilicate glass structure based on other analytical techniques, we examine here the structural and chemical factors that produce the MASS NMR spectra of our glasses and use our data to make inferences about the structure of these glasses.

TABLE 5. Fraction of ^{27}Al signal detected in representative An-Di-Fo glasses

An:Di:Fo (wt%)	Fraction detected
100:0:0	99
40:60:0	94
10:90:0	85
80:0:20	87
50:40:10	108
40:40:20	93
10:70:20	105

^{29}Si. The variation in ^{29}Si chemical shift is clearly related to the average polymerization of the glass (i.e., along a join, increasing NBO/T causes less negative chemical shifts), paralleling the variation for crystals. The ^{29}Si chemical shift also becomes less negative as the number of Al NNNs increases. In the An-Di-Fo and Cats-Di glasses, these effects oppose each other, because an increase in the amount of the framework end member (An or Cats) produces an increase in average polymerization and a simultaneous increase in the number of Al NNNs to Si. Along the join from anorthite (NBO/T = 0) to diopside (NBO/T = 2), these two effects result in a small (5 ppm) change (Fig. 3), whereas along the join from Cats (NBO/T = 0) to diopside (NBO/T = 2), the two effects virtually cancel each other (Kirkpatrick et al., 1986a). This difference is caused by Cats glass having lower Si/(Si + Al) than An glass.

Unfortunately, it appears that the signal for the different types of Si sites is not well enough resolved to allow determination of the chemical shifts, peak breadths, or relative abundance of the different types of sites. All of the spectra consist of a single, broad peak, and there are no clearly defined shoulders. Many of the peaks, in fact, can be fit to within experimental error by a single gaussian curve.

Variation in ^{29}Si NMR peak breadth is related to a number of factors, including the types of Si sites present, their

TABLE 6. ^{29}Si and ^{27}Al (11.7 T) data for samples not quenched from within 5 °C of the liquidus

Experiment no.	An:Di:Fo (wt%)	^{29}Si chemical shift (±1 ppm)	^{29}Si FWHH (±1.5 ppm)	^{29}Si left base (±4 ppm)	^{29}Si right base (±4 ppm)	^{27}Al chemical shift (±1 ppm)	^{27}Al FWHH (±1.5 ppm)
1	100:0:0	−82.6	16.3	−65	−106	—	—
2	100:0:0	−83.1	N.D.	N.D.	N.D.	—	—
3	100:0:0	−82.9	17.1	−62	−107	—	—
4	100:0:0	−82.1	16.3	−59	−107	—	—
5	100:0:0	−82.2	16.6	−62	−105	—	—
6	20:80:0	−80.2	14.7	−60	−99	58.3	19.8
7	20:80:0	−81.9	16.1	−64	−107	57.9	19.4
8	20:80:0	−80.8	15.4	−60	−102	57.3	19.2
9	40:60:0	−85.2	16.1	−66	−106	58.8	19.5
10	60:40:0	−83.6	N.D.	N.D.	N.D.	59.0	19.6

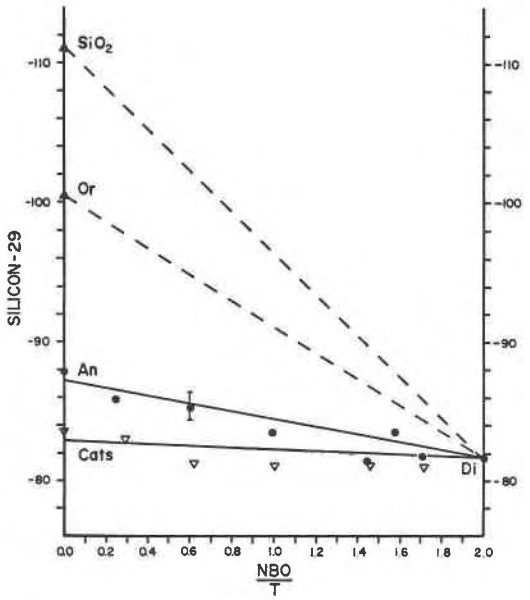

Fig. 3. Effect of average polymerization state and Al content on the ^{29}Si chemical shift of glasses (dots are An-Di glasses; hollow triangles are Cats-Di glasses). Data for the join Cats-Di is from Kirkpatrick et al. (1986a). Data for SiO_2 and Or ($KAlSi_3O_8$) from Oestrike et al. (1987b).

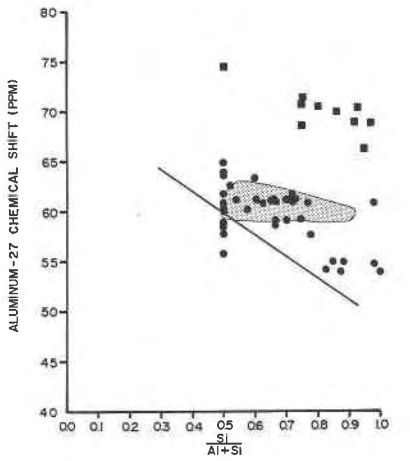

Fig. 4. Comparison of 11.7-T ^{27}Al MASS NMR chemical shifts for An-Di-Fo glasses (stippled area) to those of framework glasses (Oestrike et al., 1987b); Q^3 Al sites in crystals shown by squares, and Q^4 Al sites in crystals shown by dots. Data for crystals from Kirkpatrick et al. (1985a). See text for discussion.

characteristic peak breadth, and the nature of the large cation (Murdoch et al., 1985; Kirkpatrick et al., 1986b).

For the An-Di-Fo glasses, the lack of significant variation in peak breadth with increasing NBO/T is probably due to the less polymerized Si sites having about the same range of chemical shifts as the more polymerized sites. Because of the relatively low Si/(Si + Al), most of the Si-Q^4 sites probably have three or four Al NNN. Such sites in crystals have ^{29}Si chemical shifts in the range of -80 to -90 ppm, similar to many Q^0 to Q^3 Si sites with no ^{IV}Al NNN (Kirkpatrick et al., 1985a). This result contrasts with the results for SiO_2-$MAlO_2$ (framework) glasses and glasses along the Di-Cats join. For the framework glasses, the Si-rich and Si-poor compositions have the narrowest peaks, owing to a narrow range in the number of Al NNN to Si (Murdoch et al., 1985; Oestrike et al., 1987b). Along the Di-Cats join, on the other hand, there is a large increase in FWHH with increasing Di, owing to Cats glass having mostly Q^4(4Al) sites and Di glass having Si tetrahedra with a range of NBOs (Kirkpatrick et al., 1986a).

^{27}Al. Because the ^{27}Al spectra of the An-Di-Fo glasses contain signal for only ^{IV}Al and because the quantitation experiments demonstrate that within experimental error all Al in these glasses is detected by NMR, we conclude that within the accuracy of the NMR technique all of the Al is tetrahedrally coordinated by oxygen. This is the same conclusion reached by other recent studies of aluminosilicate glasses with M/Al > 1 (Mysen et al., 1981, 1985; Domine and Piriou, 1986; Kirkpatrick et al., 1986a). The lack of detectable Al in other than tetrahedral coordination in B-free glasses with M/Al > 1 now appears amply confirmed by a variety of methods. Based on ^{27}Al NMR data, we have reached the same conclusions for framework (SiO_2-$MAlO_2$) glasses (Oestrike et al., 1987b), as have studies using X-ray, thermochemical, and vibrational spectroscopy data (e.g., Taylor and Brown, 1979a, 1979b; Seifert et al., 1982; Navrotsky, 1986).

The relatively shielded ^{27}Al chemical shifts suggest that all or most of the Al in the An-Di-Fo glasses is partitioned into Q^4 sites. Figure 4 shows that these chemical shifts all fall in the range for Q^4 Al sites in crystalline aluminosilicates and are significantly deshielded relative to the ^{27}Al chemical shifts of Q^3 sites in phyllosilicates. The results of several Raman spectroscopic investigations also indicate that Al is preferentially concentrated into the most polymerized sites in aluminosilicate glasses (Mysen et al., 1981, 1985; Domine and Piriou, 1986). An alternative explanation of these ^{27}Al chemical shifts is that as the average NBO/T ratio increases (for instance, from zero for anorthite to two for diopside glass), the fraction of Al in non-Q^4 sites increases (also proposed by Mysen et al., 1981, 1985). By this explanation, the ^{27}Al peaks are due to overlapping signal from Q^4 and non-Q^4 sites (perhaps mostly Q^3), with the contribution from non-Q^4 sites increasing with increasing NBO/T.

Several lines of evidence suggest that the first model (Al in only Q^4 sites) is more likely to be correct. If the second model were correct (i.e., Al in both Q^4 and non-Q^4 sites), the peak width should increase as the fraction of non-Q^4 Al sites increases, because of the different chemical shifts of Q^4 and Q^3 sites. This increase does not occur. The relatively shielded ^{27}Al chemical shifts (as low as about 57 ppm) along the Cats-Di join (Kirkpatrick et al., 1986a) and the small amount of signal intensity in the range for Q^3 Al also argue against a substantial con-

centration of non-Q^4 Al. In addition, Mysen et al. (1981) interpreted their Raman spectroscopic data for glasses to indicate that for relatively low Al concentrations (less than about 6 wt% Al_2O_3), Al is strongly partitioned into Q^4 sites. This is exactly the range of compositions for which the NMR data are least conclusive. Mysen et al. (1981) did not, however, examine Mg-containing glasses.

In addition, the H_0 field dependence of the observed ^{27}Al peak maxima for our samples is small (mostly 0–1 ppm between 8.45 and 11.7 T, Table 4), indicating that the QCC of the sites dominating the peak maxima are in the range of 0–3 MHz (Ganapathy et al., 1982). For these QCCs, the peak maxima at 11.7 T are displaced only about 0 to 3 ppm from the average isotropic chemical shift. These isotropic chemical shifts are, thus, well in the range for Al in Q^4 sites. If large concentrations of Q^3 Al sites with isotropic chemical shifts of 70–75 ppm (Lippmaa et al., 1986) and QCCs of 1–3 MHz were present, their signal would be readily visible in the 67–74 ppm range. Q^3 Al sites with isotropic chemical shifts of 70–75 ppm could give the observed peak maxima of about 58–60 ppm if they had QCCs in the range of 4–6 MHz (substantially larger than observed for Q^3 Al sites in crystals). The peak maximum of such sites, however, would be 5 to 12 ppm less positive at 8.45 T than at 11.7 T, rather than the observed values of typically 0–1 ppm. Line-shape analysis of the ^{27}Al MASS NMR peak with the spinning sidebands fully removed is needed to fully define the range of QCCs in the glasses, however, and signal for some Q^3 sites could be present in the broad base of the peaks.

Thus, although the presence of some Al in non-Q^4 sites cannot be ruled out, the most straightforward interpretation of the ^{27}Al spectra of the An-Di-Fo glasses is that most of the Al is in fully polymerized Q^4 sites. For modeling the glass structures, we will assume that all of it is in Q^4.

An important implication of this conclusion for modeling glass structure is that all of our glasses, even those with NBO/T ratios approaching two, must have some fully polymerized sites into which the Al is partitioned. This conclusion is consistent with the interpretation of Raman spectra by Mysen et al. (1982), who reported the presence of fully polymerized sites in Al-free silicate glasses to a bulk NBO/T ratio of almost two.

Intermediate-range structure

The nature of the structure at greater than NNN distances in glasses (intermediate-range structure) is difficult to address using NMR data. Even if a peak can be assigned to a particular polymerization, Q^n, NMR chemical shifts are not very sensitive to structural or chemical changes beyond NNNs.

The presence of Al in dominantly Q^4 sites, however, indicates the presence of structural units at least as large as quintmers (five tetrahedra) composed of a central Al tetrahedron bonded to four Si or Al tetrahedra. If the aluminum avoidance principle (Loewenstein, 1954) holds, each quintmer would consist of an Al tetrahedron surrounded by four Si tetrahedra. The NMR data do not indicate directly whether these quintmers are separated from one another or whether they aggregate to form larger volumes that are fully polymerized.

TABLE 7. Calculated $\overline{\text{Si–O}}$ bond distances and $\angle\overline{\text{Si–O–T}}$ bond angles for anorthite-diopside-forsterite glasses

An:Di:Fo (wt%)	$\overline{\text{Si–O}}$ distance (Å) (±0.01)	$\angle\overline{\text{Si–O–T}}$ angle (°) (±1.7°)
100:0:0	1.62	134
80:20:0	1.63	133
60:40:0	1.63	133
40:60:0	1.63	131
20:80:0	1.63	130
10:90:0	1.63	130
0:100:0	1.63	130
80:10:10	1.63	132
60:30:10	1.63	132
50:40:10	1.63	131
40:50:10	1.63	131
20:70:10	1.63	130
10:80:10	1.63	129
0:90:10	1.64	129
80:0:20	1.63	131
60:20:20	1.63	130
40:40:20	1.63	129
10:70:20	1.64	129

$\angle\overline{\text{Si–O–T}}$ bond angles and $\overline{\text{Si–O}}$ bond lengths. It is not now possible to accurately calculate the NMR chemical shift of a site based on an assumed structure or to invert an observed spectrum into a structure with known bond angles and lengths from quantum-mechanical principles. For the An-Di-Fo glasses, it is not even possible to use any of the reasonably good empirical correlations between observed ^{29}Si chemical shifts and various structural parameters of materials with known structures (Higgins and Woessner, 1982; J. V. Smith and Blackwell, 1983; K. A. Smith et al., 1983; J. V. Smith et al., 1984; Mägi et al., 1984; Oldfield and Kirkpatrick, 1985). To use these correlations for individual sites in glass, one must know the chemical shift, the polymerization of the site, and the number of Al NNNs to the site. The ^{29}Si peaks for the An-Di-Fo glasses contain signal for Si sites with many different NNN environments that cannot be resolved.

It is possible, however, to obtain the average mean Si–O–T (T = Si,Al) bond angle per Si tetrahedron ($\angle\overline{\text{Si–O–T}}$) and the average mean Si–O bond length per tetrahedron ($\overline{\text{Si–O}}$) using the correlations of these parameters with ^{29}Si chemical shift for all silicates (Kirkpatrick et al., 1985a). These global correlations are not as good ($r = 0.68$ for $\angle\overline{\text{Si–O–T}}$, $r = 0.79$ for $\overline{\text{Si–O}}$) as those for the individual types of sites, but nonetheless provide useful average estimates.

For the An-Di-Fo glasses, $\angle\overline{\text{Si–O–T}}$ varies from 129° to 134°, and $\overline{\text{Si–O}}$ from 1.62 to 1.64 Å (Table 7). As expected from the calculations of Gibbs (1982) and from observations of crystalline compounds (Liebau, 1981), $\angle\overline{\text{Si–O–T}}$ decreases slightly as the glasses become less po-

lymerized. This range of $\angle\overline{\text{Si–O–T}}$ is much less than for the framework glasses, for which the $\angle\overline{\text{Si–O–T}}$ varies from 151° for SiO_2 to 135° for Cats (Oestrike et al., 1987b). As for the ^{29}Si chemical shifts, this small range most likely occurs because the Q^4 sites have a large number of Al NNNs, causing them to have mean $\angle\overline{\text{Si–O–T}}$ values in the range for less polymerized sites.

Effects of thermal history

The small differences in peak position and peak width between the spectra for the superheated and supercooled samples and those quenched from near the liquidus indicate either that the different thermal histories have little effect on melt structure or that the changes in melt structure due to changes in temperature are not preserved during quenching.

Although the ~1–2 ppm changes in the ^{29}Si chemical shift for samples with different thermal histories are within or close to analytical precision and accuracy, they are consistently in the same direction and appear to indicate that Si in these glasses becomes slightly more shielded upon superheating and slightly less shielded upon supercooling. These changes are most easily explained by a slightly larger $\angle\overline{\text{Si–O–T}}$ (more open structure or increased ring order) in the superheated samples and a smaller $\angle\overline{\text{Si–O–T}}$ (more compact structure or decreased ring order) in supercooled samples. For the compositions with the largest chemical shift differences, $An_{40}Di_{60}$ quenched from 250 °C above the liquidus and $An_{60}Di_{40}$ quenched from below the liquidus after programmed cooling, the chemical shifts are consistent with an $\angle\overline{\text{Si–O–T}}$ larger by about 1° for the superheated sample and smaller by about 1° for the supercooled sample. These changes do not appear to be due to changes in the average polymerization of the samples. Changing the polymerization would require either changing the stoichiometry of the sample (perhaps by volatilization), or changing the coordination of one or more components of the glass (e.g., formation of ^{VI}Al or changing the abundance of O^{2-}), neither of which we observe.

Structural models

The results of many studies using a variety of analytical techniques (including viscosity and density measurements, Raman spectroscopy, and NMR spectroscopy) are consistent with the conclusion that silicate liquids and glasses with M/Al ≥ 1 contain tetrahedral Si sites with a range of polymerizations (Bockris et al., 1956; Masson, 1972; Brawer and White, 1975; Virgo et al., 1980; Mysen et al., 1980, 1981, 1982, 1985; Domine and Piriou, 1983; McMillan, 1984a, 1984b; Grimmer et al., 1984; Engelhardt et al., 1985; Dupree et al., 1984). We present here a new technique for examining the Si/(Si + Al) ratio of the Q^4 sites and the extent of polymerization of the non-Q^4 sites by modeling ^{27}Al MAS NMR spectra. This technique makes use of ^{27}Al data for SiO_2-$MAlO_2$ (framework) glasses, which contain only fully polymerized sites (Oestrike et al., 1987b). For these glasses, the 11.7-T ^{27}Al peak maxima become less shielded with decreasing Si/(Si + Al), following a linear relationship (Fig. 4), and do not depend very much on the nature of the large cation (±1 to 2 ppm).

The average Si/(Si + Al) ratio of the fully polymerized (Q^4) sites in glasses with M/Al ≥ 1 can be determined if, as concluded above, all Al is partitioned into Q^4 sites. Figures 5A and 5B show the variation of the ^{27}Al chemical shifts vs. bulk Si/(Si + Al) for glasses along the joins An-Di and Cats-Di and compare them with the relationship for framework glasses. For both An-Di and Cats-Di, the ^{27}Al peak maxima diverge from the framework-glass trend, but remain in the field of chemical shifts of Q^4 sites in crystals (see also Fig. 4).

In our model, glasses for which the ^{27}Al chemical shifts fall off of the framework-glass line are composed of relatively Al-rich Q^4 sites (for which the chemical shifts are assumed to plot on the framework-glass line) and Al-free, less polymerized sites. Thus, along the join An-Di, the average Si/(Si + Al) ratio of the Q^4 sites remains about 0.5. Even $An_{10}Di_{90}$ glass, then, has Q^4 sites with an average Si/(Al + Si) ratio of about 0.5. For the An-Di-Fo glasses with 10 and 20 wt% Fo, the ^{27}Al chemical shifts are also nearly the same as that for anorthite glass, again indicating that Q^4 sites in these glasses have an average Si/(Si + Al) ratio of about 0.5 (Table 4). For glasses along the join Cats-Di, however, the ^{27}Al chemical shifts become more shielded with increasing Si/(Si + Al). Along this join, the average Si/(Si + Al) ratio for the Q^4 sites varies from about 0.3 for Cats glass to about 0.7 for $Cats_{10}Di_{90}$ glass (Fig. 5B).

It is possible to model the percentage of the total tetrahedral sites that are Q^4 and to estimate the average polymerization of non-Q^4 sites using the ^{27}Al chemical shifts by making the following assumptions: (1) All Al is in tetrahedral coordination. (2) All Al is segregated into Q^4 sites. (3) The glass samples are anhydrous. (4) There is no oxygen not coordinated to a tetrahedral cation (nontetrahedral oxygen). (5) The correlation of ^{27}Al chemical shifts with Si/(Si + Al) for framework glass (Oestrike et al., 1987b) is valid for Q^4 sites in all aluminosilicate glasses. Assumptions 1 and 2 are based on data presented in earlier sections of this paper. We believe assumption 3 to be correct to a close approximation, because the glasses were prepared under anhydrous conditions. Although nontetrahedral oxygen has been observed in glasses and melts, the concentration is very low for compositions more polymerized than NBO/T = 2 (Mysen et al., 1982; Semkow and Haskin, 1985). The glasses of this study have NBO/T ratios of from 0 to 2, and we believe, therefore, that assumption 4 is also good to a close approximation. Assumption 5 is based on the concept that ^{27}Al NMR chemical shifts are functions of the local environment only (i.e., NN and NNN) and has much empirical support (Lippmaa et al., 1981; K. A. Smith et al., 1983).

Figure 6 presents the calculated results for the An-Di glasses, as described in Appendix 1. The diagonal line is the observed correlation for framework glasses (Oestrike

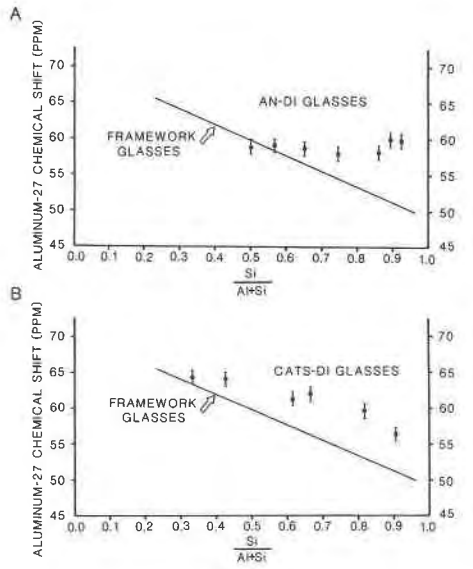

Fig. 5. Comparison of 11.7-T ^{27}Al MASS NMR chemical shifts for An-Di glasses (**A**) and Cats-Di glasses (**B**) with those of framework glasses (Oestrike et al., 1987b).

et al., 1987b), and each curved line gives the predicted ^{27}Al peak position for a given average Q^n of the nonframework sites (the number next to the curve). Thus, the upper curve, labeled 3.0, represents a model assuming the presence of only Q^4 and Q^3 sites, and the lower curve, labeled 1.0, a model assuming the presence of only Q^4 and Q^1 sites. The horizontal line represents a model that assumes Q^4 sites and nonframework sites with an *average* polymerization of Q^2. Above this line there are fewer Q^4 sites than for a simple mechanical mixture of An and Di, whereas below it there are more Q^4 sites than for a mechanical mixture.

Figure 6 shows that glasses in the system An-Di appear to contain Q^4 sites with a Si/(Si + Al) ratio of 0.5 ± 0.1 (about the same as crystalline anorthite) and a nonframework component with an average polymerization of about Q^2. Unfortunately, this model does not provide information about the speciation of the nonframework sites, only the *average* polymerization state.

Figure 7 shows similar model relationships for glasses along the join Cats-Di (data from Kirkpatrick et al., 1986a). Once again, the straight diagonal line is the correlation for the framework glasses, and the curved lines are predicted chemical shifts for a particular average polymerization, Q^n, of the non-Q^4 sites. For glasses in this system, the observed chemical shifts fall below the horizontal line, indicating that the Q^4 sites are more abundant than they would be in a mechanical mixture of Cats and Di. The average polymerization for the non-Q^4 sites is about $Q^{1.7}$. For glasses in both the systems An-Di and Cats-Di, the average polymerization of the non-Q^4 sites remains constant (about $Q^{2.0}$ for An-Di and about $Q^{1.7}$ for Cats-Di). The Si/(Si + Al) ratio of the Q^4 sites in the

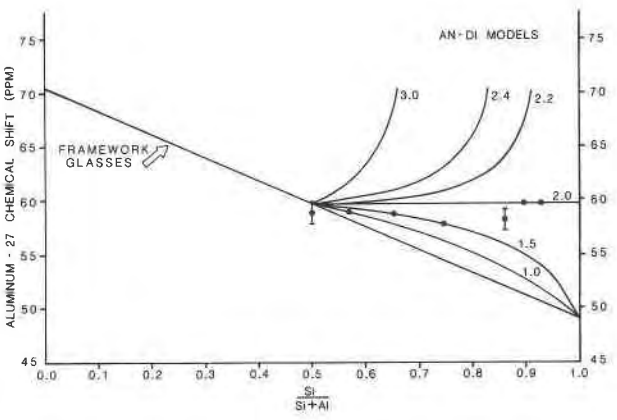

Fig. 6. Comparison of the 11.7-T ^{27}Al MASS NMR chemical shifts for An-Di glasses to the calculated chemical shifts of various assumed glass structures (see text and App. 1).

Cats-Di glasses may increase with increasing bulk Si/(Si + Al) to reduce the number of Al–O–Al linkages.

CONCLUSIONS

The data and modeling presented above provide insight into the structure of aluminosilicate glasses and the applicability of MASS NMR to the study of glasses. The main conclusions of this work are as follows:

1. It is not possible to resolve signals from different types of Si sites in any of the glasses studied here using ^{29}Si MASS NMR spectroscopy. Each ^{29}Si spectrum consists of a broad featureless peak.

2. The average shielding at Si decreases as the average number of bridging oxygens decreases, parallel to the trend for crystals and for glasses in the system CaO-Al_2O_3-SiO_2. This variation reflects the increasing contribution of the non-Q^4 Si sites to the less shielded portion of the broad ^{29}Si peak.

3. Detailed structural information, such as the relative proportions of Si in different polymerization states or the

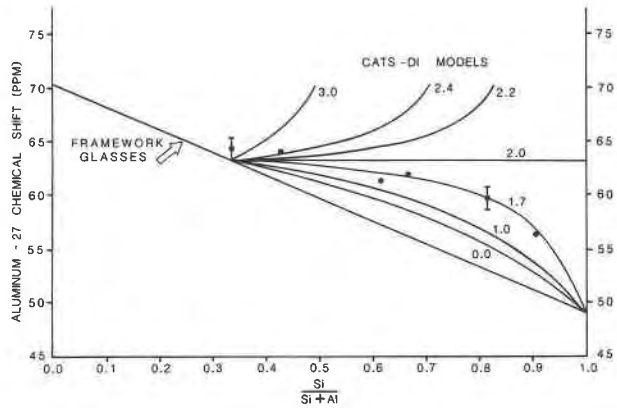

Fig. 7. Comparison of the 11.7-T ^{27}Al MASS NMR chemical shifts for Cats-Di glasses to the calculated chemical shifts of various assumed glass structures (see text and App. 1).

relative proportions of Si with different numbers of NNN Al, is difficult to obtain directly from the ^{29}Si data, because the peak position and breadth are the result of several factors, including bond-angle and bond-length disorder, Al-Si disorder, and polymerization-state disorder. It is not at present possible to determine the extent of peak broadening caused by each of these different effects.

4. Essentially all the Al in these glasses is detectable by ^{27}Al MASS NMR at 11.7 T and is in tetrahedral sites. Most of it appears to be in fully polymerized, Q^4, sites.

5. It is not possible to resolve signals for different types of Al sites (for instance Q^4 Al with different numbers of Al NNNs) in any of the glasses studied here using ^{27}Al MASS NMR spectroscopy. Each ^{27}Al spectrum consists of a single broad peak.

6. The average mean Si–O–T bond angle and average mean Si–O bond length for An-Di-Fo glasses are about 132° ± 3° and 1.63 ± 0.01 Å, as estimated from ^{29}Si chemical-shift correlations for all types of Si sites in crystals. Estimates calculated in this way are expected to be less accurate than the estimates for framework glasses, which contain only Q^4 sites (Oestrike et al., 1987b).

7. Assuming that all Al is in Q^4 sites, the average Si/(Si + Al) ratio of the Q^4 sites in An-Di-Fo glasses is constant at 0.5 ± 0.1. The average Si/(Si + Al) ratio of the Q^4 sites along the join Cats-Di, however, varies from about 0.3 for Cats glass to about 0.7 for $Cats_{10}Di_{90}$ glass.

8. Structural models indicate that the abundance of Q^4 sites in glasses along the join An-Di is approximately equal to the abundance expected for a mechanical mixture of An and Di, whereas the abundance of Q^4 sites in glasses along with the join Cats-Di is greater than expected for a mechanical mixture of Cats and Di.

9. These models also indicate that the average polymerization of the non-Q^4 sites along the join An-Di is roughly Q^2, whereas the average polymerization of non-Q^4 sites along the join Cats-Di is roughly $Q^{1.7}$.

10. The effects of differing thermal histories on the MASS NMR spectra of our glasses are very small, mostly within experimental error. What changes there are indicate that Si in glasses along the join An-Di is slightly more shielded upon superheating and slightly less shielded upon supercooling, consistent with an increase in $\angle\overline{\text{Si–O–T}}$ with superheating and a decrease with supercooling.

11. Superheated samples have a slightly increased ^{29}Si peak width, consistent with slightly more structural disorder than for glasses quenched from or below the liquidus, but as for the peak maxima, the observed differences are close to the experimental precision and accuracy.

ACKNOWLEDGMENTS

We wish to thank Ben Montez, Charles A. Weiss, Jr., Wang-Hong Yang, Gary Turner, and Eric Oldfield for much useful discussion. D. M. Henderson, J. Bass, D. E. Anderson, and Bjorn Mysen reviewed earlier versions of the manuscript, greatly improving it. Cameron Begg helped with the electron-microprobe analysis, and Y. Aoki provided the diopside glass samples that were program-cooled. This research was supported by NSF grants EAR-8218741, EAR-8207260, and EAR-8408421.

REFERENCES CITED

Andrew, E.R. (1971) The narrowing of NMR spectra of solids by high-speed specimen rotation and the resolution of chemical shift in spin multiple structures for solids. Progress in NMR Spectroscopy, 8, 1–39.

Angell, C.A. (1985) Spectroscopy simulation and scattering, and the medium range order problem in glass. Journal of Non-Crystalline Solids, 73, 1–17.

Bockris, J.O'M., Tomlinson, J.W., and White, J.L. (1956) The structure of the liquid silicates: Partial molar volumes and expansivities. Transactions of the Faraday Society, 52, 299–310.

Brawer, S. (1985) Relaxation in viscous liquids and glasses: A review of phenomenology, molecular dynamic simulations, and theoretical treatment, 220 p. American Ceramic Society, Inc., Columbus, Ohio.

Brawer, S.A., and White, W.B. (1975) Raman spectroscopic investigations of the structure of silicate glasses. 1. The binary alkali silicates. Journal of Chemical Physics, 63, 2421–2432.

Bray, P.J. (1985) Nuclear magnetic resonance studies of glass structure. Journal of Non-Crystalline Solids, 73, 19–45.

Brown, I.D., and Shannon, R.D. (1973) Empirical bond-strength–bond-length curves for oxides. Acta Crystallographica, A29, 266–282.

Carmichael, I.S.E. (1979) Glass and the glassy rocks. *In* H.S. Yoder, Ed., The evolution of the igneous rocks, fiftieth anniversary perspectives, p. 233–244. Princeton University Press, Princeton, N.J.

DeJong, B.H.W.S., Schramm, C.M., and Parziale, V.E. (1984) Polymerization of silicate and aluminate tetrahedra in glasses, melts, and aqueous solutions—V. The polymeric structure of silica in albite and anorthite composition glass and the devitrification of amorphous anorthite. Geochimica et Cosmochimica Acta, 48, 2619–2629.

Domine, F., and Piriou, B. (1983) Study of sodium silicate melt and glass by infrared reflectance spectroscopy. Journal of Non-Crystalline Solids, 55, 125–130.

——— (1986) Raman spectroscopic study of the SiO_2-Al_2O_3-K_2O vitreous system: Distribution of silicion second neighbors. American Mineralogist, 71, 38–50.

Dupree, R., Holland, D., McMillan, P.W., and Pettifer, R.F. (1984) The structure of soda-silica glasses: A MAS NMR study. Journal of Non-Crystalline Soilds, 68, 399–410.

Dupree, R., Holland, D., and Williams, D.S. (1985) An examination by magic angle spinning NMR of the changes in the environment of ^{27}Al during the devitrification of an aluminoborate glass. Physics and Chemistry of Glasses, 26, 50–52.

Engelhardt, G., Nofz, M., Forkel, K., Wihsmann, F.G., Mägi, M., Samoson, A., and Lippmaa, E. (1985) Structural studies of calcium aluminosilicate glasses by high-resolution solid-state ^{29}Si and ^{27}Al magic angle spinning nuclear magnetic resonance. Physics and Chemistry of Glasses, 26, 157–165.

Fenzke, D., Freude, D., Frohlick, T., and Haase, J. (1984) NMR intensity measurements of half-integer quadrupole nuclei. Chemical Physics Letters, 111, 171–175.

Fyfe, C.A., Gobbi, G.C., Hartman, J.S., Klinowski, J., and Thomas, J.M. (1982a) Solid-state magic-angle spinning aluminum-27 nuclear magnetic resonance studies of zeolites using a 400 MHz high-resolution spectrometer. Journal of Physical Chemistry, 86, 1247–1250.

Fyfe, C.A., Gobbi, G.C., Klinowski, J.M., Thomas, J.M., and Ramadas, S. (1982b) Resolving crystallographically distinct tetrahedral sites in silicate and ZSM-5 by solid-state NMR. Nature, 296, 530–533.

Ganapathy, S., Schramm, S., and Oldfield, E. (1982) Variable-angle sample-spinning high resolution NMR of solids. Journal of Chemical Physics, 77, 4360–4365.

Gibbs, G.V. (1982) Molecules as models for bonding in silicates. American Mineralogist, 67, 421–450.

Grimmer, A.R., Mägi, M., Hahneat, M., Stade, H., Samoson, A., Wieker, W., and Lippmaa, E. (1984) High-resolution solid-state ^{29}Si nuclear magnetic resonance spectroscopic studies of binary alkali silicate glasses. Physics and Chemistry of Glasses, 25, 105–109.

Higgins, J.B., and Woessner, D.E. (1982) ^{29}Si, ^{27}Al, and ^{23}Na NMR spectra of framework silicates (abs.). EOS, 63, 1139.

Janes, N., and Oldfield, E. (1985) Prediction of silicon-29 NMR chemical

shifts using a group electronegativity approach: Applications to silicate and aluminosilicate structures. Journal of the American Chemical Society, 107, 6769–6775.

Kinsey, R.A., Kirkpatrick, R.J., Hower, J., Smith, K.A., and Oldfield, E. (1985) High resolution aluminum-27 and silicon-29 nuclear magnetic resonance spectroscopic study of layer silicates, including clay minerals. American Mineralogist, 70, 537–548.

Kirkpatrick, R.J., Smith, K.A., Schramm, S., Turner, G., and Yang, W.H. (1985a) Solid-state nuclear magnetic resonance spectroscopy of minerals. Annual Review of Earth and Planetary Science, 13, 29–47.

Kirkpatrick, R.J., Kinsey, R.A., Smith, K.A., Henderson, D.M., and Oldfield, E. (1985b) High-resolution solid-state sodium-23, aluminum-27, and silicon-29 nuclear magnetic resonance spectroscopic reconnaissance of alkali and plagioclase feldspars. American Mineralogist, 70, 106–123.

Kirkpatrick, R.J., Oestrike, R., Weiss, C.A., Jr., Smith, K.A., and Oldfield, E. (1986a) High-resolution ^{27}Al and ^{29}Si NMR spectroscopy of glasses and crystals along the join $CaMgSi_2O_6$-$CaAl_2SiO_6$. American Mineralogist, 71, 705–711.

Kirkpatrick, R.J., Dunn, T., Schramm, S., Smith, K.A., Oestrike, R., and Turner, G. (1986b) Magic angle sample spinning nuclear magnetic resonance spectroscopy of silicate glasses: A review. *In* A.G. Revesz and G.E. Walrafen, Eds., Structure and bonding in non-crystalline solids. U.S. National Bureau of Standards, Washington, D.C.

Lacey, E.D. (1963) Aluminum in glasses and in melts. Physics and Chemistry of Glasses, 4, 234–238.

Liebau, F. (1981) The influence of cation properties on the conformation of silicate and phosphate anions. *In* M. O'Keeffe and A. Navrotsky, Eds., Structure and bonding in crystals II, p. 197–232. Academic Press, New York.

Lippmaa, E., Mägi, M., Samoson, A., Engelhardt, G., and Grimmer, A.R. (1980) Structural studies of silicates by solid-state high-resolution ^{29}Si NMR. Journal of the American Chemical Society, 102, 4889–4893.

Lippmaa, E., Mägi, M., Samoson, A., Tarmak, M., and Engelhardt, G. (1981) Investigation of the structure of zeolites by solid-state high-resolution ^{29}Si NMR spectroscopy. Journal of the American Chemical Society, 103, 4992–4996.

Lippmaa, E., Samoson, A., and Mägi, M. (1986) High-resolution ^{27}Al NMR of aluminosilicates. Journal of the American Chemical Society, 108, 1730–1735.

Loewenstein, W. (1954) The distribution of aluminum in the tetrahedra of silicates and aluminates. American Mineralogist, 39, 92–96.

Mägi, M., Lippmaa, E., Samoson, A., Engelhardt, G., and Grimmer, A.R. (1984) Solid-state high resolution silicon-29 chemical shifts in silicates. Journal of Physical Chemistry, 88, 1518–1522.

Masson, C.R. (1972) Thermodynamics and constitution of silicate slags. Journal of the Iron and Steel Institute, February, 89–96.

McMillan, P. (1984a) Structural studies of silicate glass and melts—Applications and limitations of Raman spectroscopy. American Mineralogist, 69, 622–644.

——— (1984b) A Raman spectroscopic study of glasses in the system CaO-MgO-SiO_2. American Mineralogist, 69, 645–659.

Müller, D., Gessner, W., Behrens, H.J., and Scheler, G. (1981) Determination of the aluminum coordination in aluminum-oxygen compounds by solid-state high-resolution ^{27}Al NMR. Chemical Physics Letters, 79, 59–62.

Murdoch, J.B., Stebbins, J.F., and Carmichael, I.S.E. (1985) High-resolution ^{29}Si NMR study of silicate and aluminosilicate glasses. The effect of network-modifying cations. American Mineralogist, 70, 332–343.

Mysen, B.O., Virgo, D., and Scarfe, C.M. (1980) Relations between the anionic structure and viscosity of silicate melts—A Raman spectroscopic study. American Mineralogist, 65, 690–710.

Mysen, B.O., Virgo, D., and Kushiro, I. (1981) The structural role of aluminum in silicate melts—A Raman spectroscopic study at 1 atmosphere. American Mineralogist, 66, 678–701.

Mysen, B.O., Virgo, D., and Seifert, F.A. (1982) The structure of silicate melts: Implications for chemical and physical properties of natural magma. Review of Geophysics and Space Physics, 20, 353–383.

——— (1984) Redox equilibria of iron in alkaline earth silicate melts: Relationships between melt structure, oxygen fugacity, temperature and properties of iron-bearing silicate liquids. American Mineralogist, 69, 834–847.

——— (1985) Relationships between properties and structure of aluminosilicate melts. American Mineralogist, 70, 88–105.

Navrotsky, A. (1981) Thermodynamics of mixing in silicate glasses and melts. In R.C. Newton, A. Navrotsky, and B.J. Wood, Eds., Thermodynamics of minerals and melts, vol. 1, p. 189–205. Springer-Verlag, New York.

——— (1986) Thermodynamics of silicate melts and glasses. Mineralogical Association of Canada Short Course Handbook, 12, 130–153.

Oestrike, R., Navrotsky, A., Turner, G.L., Montez, B., and Kirkpatrick, R.J. (1987a) Structural environment of Al dissolved in 2PbO-B_2O_3 glasses used for solution calorimetry: An ^{27}Al NMR study. American Mineralogist, 72, 788–791.

Oestrike, R., Yang, W.H., Weiss, C.A., Kirkpatrick, R.J., Hervig, R.L., Navrotsky, A., and Montez, B. (1987b) High-resolution ^{23}Na, ^{27}Al, and ^{29}Si NMR spectroscopy of framework aluminosilicate glasses. Geochimica et Cosmochimica Acta, 51, 2199–2209.

Oldfield, E., and Kirkpatrick, R.J. (1985) High-resolution NMR of inorganic solids. Science, 227, 1537–1544.

Osborn, E.F., and Tait, D.B. (1952) The system diopside-forsterite-anorthite. American Journal of Science, 252, 413–433.

Randall, J.T., Rooksby, H.P., and Cooper, B.S. (1930) X-ray diffraction and the structure of vitreous solids—1. Zeitschrift für Kristallographie, Kristallgeometrie, Kristallphysik und Kristallchemie, 75, 196–215.

Richet, P., and Bottinga, Y. (1984) Anorthite, andesine, wollastonite, diopside, cordierite, and pyrope: Thermodynamics of melting, glass transitions, and properties of the amorphous phases. Earth and Planetary Science Letters, 67, 415–432.

——— (1986) Thermochemical properties of silicate glasses and liquids: A review. Reviews of Geophysics, 24, 1–25.

Riebling, E.F. (1967) Structural relationships between the liquid and glass states for binary and ternary oxide systems: A density study. Revue Internacionale de Hautes Temperatures et des Refractaires, 4, 65–76.

Risbud, S., Kirkpatrick, R.J., Taglialavore, A.P., and Montez, B. (1987) Solid-state NMR evidence of 4-, 5-, and 6-fold aluminum sites in roller-quenched SiO_2-Al_2O_3 glasses. Journal of the American Ceramic Society, 70, C10–C12.

Schmidt, V.H. (1971) Pulse response in the presence of quadrupolar splitting. Proceedings of the Ampere International Summer School II, Yugoslavia, 75–83.

Seifert, F.A., Mysen, B.O., and Virgo, D. (1981) Structural similarity of glasses and melts relevant to petrological processes. Geochimica et Cosmochimica Acta, 45, 1879–1884.

——— (1982) Three-dimensional network structure of quenched melts (glass) in the systems SiO_2-$NaAlO_2$, SiO_2-$CaAl_2O_4$ and SiO_2-$MgAl_2O_4$. American Mineralogist, 67, 696–717.

Semkow, K.W., and Haskin, L.A. (1985) Concentrations and behavior of oxygen and oxide ion in melts of composition CaO-MgO-$XSiO_2$. Geochimica et Cosmochimica Acta, 49, 1897–1908.

Smith, J.V., and Blackwell, C.S. (1983) Nuclear magnetic resonance of silica polymorphs. Nature, 303, 223–225.

Smith, J.V., Blackwell, C.S., and Hovis, G.L. (1984) NMR of albite-microcline series. Nature, 309, 140–142.

Smith, K.A., Kirkpatrick, R.J., Oldfield, E., and Henderson, D.M. (1983) High-resolution silicon-29 nuclear magnetic resonance spectroscopic study of rock-forming silicates. American Mineralogist, 68, 1206–1215.

Taylor, M., and Brown, G.E., Jr. (1979a) Structure of mineral glasses—I. The feldspar glasses $NaAlSi_3O_8$, $KAlSi_3O_8$. Geochimica et Cosmochimica Acta, 43, 61–75.

——— (1979b) Structure of mineral glasses—II. The SiO_2-$NaAlSiO_4$ join. Geochimica et Cosmochimica Acta, 43, 1467–1473.

Taylor, M., Brown, G.E., and Fenn, P.M. (1980) Structure of mineral glasses—III. $NaAlSi_3O_8$ supercooled liquid at 805°C and the effects of thermal history. Geochimica et Cosmochimica Acta, 44, 109–117.

Thomas, J.M., Klinowski, J., Ramadas, S., Anderson, M.W., Fyfe, G.A., and Gobbi, G.C. (1983a) New approaches to the structural characterization of zeolites: Magic-angle spinning NMR (MASNMR). *In* G.D. Stucky and F.G. Dwyer, Eds., Intrazeolite chemistry, p. 159–180. American Chemical Society, Washington, D.C.

Thomas, J.M., Klinowski, J., Ramadas, S., Hunter, B.K., and Tennakoon, D.T.B. (1983b) The evaluation of non-equivalent tetrahedral sites from ^{29}Si NMR chemical shifts in zeolites and related alumino-silicates. Chemical Physics Letters, 102, 158–162.

Virgo, D., Mysen, B.O., and Kushiro, I. (1980) Anionic constitution of 1-atmosphere silicate melts: Implications for the structure of igneous melts. Science, 208, 1371–1373.

Waseda, Y., and Toguri, J.M. (1977) The structure of molten binary silicate systems $CaO-SiO_2$ and $MgO-SiO_2$. Metallurgical Transactions B, 8B, 563–568.

Wonnacott, R.J., and Wonnacott, T.H. (1970) Econometrics. Wiley, New York, 445 p.

MANUSCRIPT RECEIVED SEPTEMBER 21, 1987
MANUSCRIPT ACCEPTED JANUARY 22, 1988

APPENDIX 1. STRUCTURAL MODEL CALCULATIONS

The model calculations presented in this paper (Figs. 6 and 7) use the calculated values for the average Si/(Si + Al) ratio, the calculated average NBO/T ratio (Mysen et al., 1982, 1984, 1985), and assumptions 1 to 5 in the text. We use the Q^n notation and the NBO/T ratio interchangeably, because both are measures of polymerization state and are related by the expression NBO/T = $4 - n$.

The average number of nonbridging oxygens per tetrahedron is

$$\text{NBO/T} = [(2 \times \text{O}) - (4 \times \text{T})]/\text{T}, \qquad \text{(A1)}$$

(Mysen et al., 1984), where O is the fraction of oxygen atoms in the glass and T is the fraction of atoms in the glass that are in tetrahedral coordination. Thus, for the composition SiO_2, NBO/T = $[(2 \times 2)/3 - (4 \times 1)/3]/(1/3) = 0$, and for the composition Mg_2SiO_4, NBO/T = $[(2 \times 4)/7 - (4 \times 1)/7]/(1/7) = 4$.

All Al in the glasses studied here is in tetrahedral coordination. Thus, we assume T in Equation A1 is the fraction of Si plus Al atoms. Although O^{2-} has been observed in some glasses, it appears to have a very low concentration in glasses more polymerized than NBO/T = 2 (Mysen et al., 1982; Semkow and Haskin, 1985). Because the glasses in this study have NBO/T ratios of from 0 to 2, we assume that there is no O^{2-} in these glasses. Using these assumptions, the NBO/T ratio can be calculated for any glass composition studied here. For example, the weight percent compositions $An_{80}Di_{20}$ and $An_{20}Di_{80}$ have NBO/T ratios of 0.28 and 1.44, respectively.

The average Si/(Si + Al) ratio can be calculated without assumptions if the composition of the glass is known accurately. For example, the weight percent compositions $An_{80}Di_{20}$ and $An_{20}Di_{80}$ have average Si/(Si + Al) ratios of 0.57 and 0.86, respectively.

All the glasses studied here have ^{27}Al chemical shifts in the range of Q^4 Al. Therefore, given our assumptions, the glasses that are not fully polymerized consist of a mixture of Q^4 sites and non-Q^4 sites. For instance, $An_{80}Di_{20}$ glass (NBO/T = 0.28) is assumed to be composed of Q^4 sites (NBO/T = 0) and non-Q^4 sites (NBO/T > 0.28) in proportions such that the bulk NBO/T ratio is 0.28.

For a given bulk NBO/T ratio, a series of glass configurations can be considered each with a different NBO/T ratio of the non-Q^4 sites. The fraction of each type of site can be calculated from the expression

$$\text{NBO/T (total)} = X(\text{NBO/T of } Q^4) + (1 - X)(\text{NBO/T of } Q^n), \qquad \text{(A2)}$$

where X is the atom fraction of tetrahedral sites that are Q^4 sites and n is the average number of bridging oxygens per tetrahedron of the non-Q^4 sites. For example, one possible configuration would consist of Q^4 sites (NBO/T = 0) and Q^0 sites (NBO/T = 4). For the composition $An_{80}Di_{20}$, this configuration yields 93% Q^4 tetrahedra and 7% Q^0 tetrahedra. Similarly, a configuration consisting of Q^4 sites and an *average* non-Q^4 polymerization of $Q^{2.4}$, would consist of 82.5% Q^4 and 17.5% $Q^{2.4}$.

If all of the Al is in Q^4 sites, the Si/(Si + Al) ratio of the Q^4 sites can be calculated for each possible configuration and a given composition. The Si/(Si + Al) ratio of the Q^4 sites can be expressed as the percentage of Si atoms in Q^4 sites divided by the sum of the percentages of Al and Si atoms in Q^4 sites. The percentage of Si atoms in Q^4 sites is the percentage of tetrahedra that are Si minus the percentage of non-Q^4 tetrahedra. For the composition $An_{80}Di_{20}$ with an assumed configuration of Q^4 and Q^3 sites only, the percentage of Si atoms in Q^4 sites is 57% [the percentage of tetrahedra that are Si tetrahedra for a Si/(Si + Al) ratio of 0.57] minus 28% (the percentage of tetrahedra that are non-Q^4) = 29%. The percentage of Al in the Q^4 sites is simply the percentage of tetrahedra that are Al tetrahedra, because it is assumed that all Al is in Q^4 sites. Thus, for composition $An_{80}Di_{20}$, the percentage of tetrahedra that are Al is 43% [the percentage of tetrahedra that are Al tetrahedra for Si/(Si + Al) = 0.57]. Therefore, for this composition with an assumed configuration consisting of only Q^4 and Q^3 sites, the Si/(Si + Al) ratio of the Q^4 sites is 29/(43 + 29) = 0.40.

Calculating the Si/(Si + Al) ratio of the Q^4 sites automatically predicts the ^{27}Al chemical shift of Q^4 sites since they are assumed to follow the simple linear relationship observed for framework glasses

$$\delta^{27}\text{Al} = -21.6[\text{Si}/(\text{Si} + \text{Al})] + 70.5 \qquad \text{(A3)}$$

with $r^2 = 0.96$ (Oestrike et al., 1987b). As shown above, the Si/(Si + Al) ratio of the composition $An_{80}Di_{20}$ with a configuration consisting of only Q^4 and Q^3 sites is 0.40. Thus, the predicted ^{27}Al chemical shift is 61.9 ppm.

Calculation of the Si/(Si + Al) ratios of the Q^4 sites for a given configuration along a series of compositions with differing average Si/(Si + Al) ratios combined with Equation A3 yields the predicted trajectory of ^{27}Al chemical shifts for that configuration and range of compositions. The curved lines in Figures 6 and 7 are these predicted trajectories. The number on each trajectory indicates the Q value of the non-Q^4 sites for that particular assumed configuration. The line labeled 2.4, for instance, is the calculated ^{27}Al trajectory for an assumed configuration of Q^4 and non-Q^4 sites with, on average, $Q^{2.4}$ polymerization.